





Article

Unexpected Light-Induced Thermal Hysteresis in Matrix Embedded Low Cooperative Spin Crossover Microparticles

Diana Plesca ¹, Anastasia Railean ¹, Radu Tanasa ¹, Alexandru Stancu ¹, Jérôme Laisney ², Marie-Laure Boillot ² and Cristian Enachescu ^{1,*}

¹ Faculty of Physics, Alexandru Ioan Cuza University, 700506 Iasi, Romania; diana.plesca@student.uaic.ro (D.P.); anastasia.railean@student.uaic.ro (A.R.); radu.tanasa@uaic.ro (R.T.); alstancu@uaic.ro (A.S.)

² Institut de Chimie Moléculaire et des Matériaux d'Orsay, Université Paris-Saclay, CNRS, UMR 8182, CEDEX, 91405 Orsay, France; Jerome.Laisney@uky.edu (J.L.); marie-laure.boillot@universite-paris-saclay.fr (M.-L.B.)

* Correspondence: cristian.enachescu@uaic.ro

Abstract: The embedding of spin-crossover micro- or nanocrystals in various surroundings dramatically changes their functionalities based on first-order spin transitions. The dampening of their internal cooperativity, together with introducing a new kind of interactions occurring at interfaces between spin-crossover particles and their environment, results in spectacular effects, as an enhanced hysteresis with non-cooperative transitions. In this work, we deal with the influence of the embedding matrix on the light-induced thermal hysteresis (LITH) in the case of spin-crossover microparticles of $\text{Fe}(\text{phen})_2(\text{NCS})_2$. Despite the low cooperativity of this compound, the competition between the continuous photoexcitation towards the metastable high spin state and the relaxation down to low spin ground state leads to a light-induced thermal hysteresis, with a quasi-static width of around 10 K. This unexpected hysteresis is explained by considering a switch-on/cutoff mechanism of the particle-matrix interactions in the framework of a mean-field approach based on negative external pressures, with Gaussian distributed variations and of an Ising-like model with various interactions with the environment. Additional first-order reversal curves measurements and corresponding calculated distributions are in line with relaxations under light and confirm the existence of a non-kinetic LITH.

Keywords: spin-crossover; light-induced; hysteresis; first-order reversal curves; glycerol matrix



Citation: Plesca, D.; Railean, A.; Tanasa, R.; Stancu, A.; Laisney, J.; Boillot, M.-L.; Enachescu, C. Unexpected Light-Induced Thermal Hysteresis in Matrix Embedded Low Cooperative Spin Crossover Microparticles. *Magnetochemistry* **2021**, *7*, 59. <https://doi.org/10.3390/magnetochemistry7050059>

Academic Editor: Marilena Ferbinteanu

Received: 5 April 2021
Accepted: 27 April 2021
Published: 29 April 2021

Publisher's Note: MDPI stays neutral with regard to jurisdictional claims in published maps and institutional affiliations.



Copyright: © 2021 by the authors. Licensee MDPI, Basel, Switzerland. This article is an open access article distributed under the terms and conditions of the Creative Commons Attribution (CC BY) license (<https://creativecommons.org/licenses/by/4.0/>).

1. Introduction

Among multiple kinds of hysteresis observed in spin-crossover compounds, light-induced thermal hysteresis (LITH) is maybe the most spectacular. Its discovery was made more than twenty years ago [1,2], even if its existence has been predicted some years earlier in the form of a hysteresis under light irradiation [3], marking a new stage in the study of these intriguing compounds and opening the possibility for all optical memories [4].

The main underlying processes for LITH are the light excitation, which may trigger the switching between the low spin (LS) state and the metastable high spin (HS) state, a phenomenon known as light-induced excited spin state trapping (LIESST) [5,6] and the subsequent relaxation towards the LS ground state [7]. LITH is, therefore, the result of the competition between photoexcitation and relaxation in the temperature domain below the thermal transition. At low temperatures, the photoexcitation dominates as the relaxation, either thermally activated or in the tunneling regime, occurs slowly, and consequently, the compound preserves its HS state. However, at somewhat higher temperatures—but still below thermal transition temperatures—relaxation takes over, and the compound switches to the LS state. In between, there is a temperature range in which the bistability is present [8].

To understand what singles out the LITH, we should first refer to the thermal behavior of spin-crossover compounds. The thermal transition between the undegenerated LS state

stable at low temperatures to the highly degenerated HS state, stable at high-temperature is accompanied by a hysteresis, namely thermal hysteresis (TH) if the intermolecular interactions of elastic origin are higher than a threshold. At the temperatures where the thermal transition takes place, for most of the spin-crossover compounds, the relaxation between the two states is very fast (nanoseconds, which is faster than experimental time) and, consequently, in most situation, the thermal hysteresis can be considered in a first approximation as rate-independent (with some exceptions observed in nanoparticles or compounds with low transition temperatures [9]). In the case of LITH, both the photoexcitation and the relaxation are kinetic processes, occurring simultaneously with the experimental time. Therefore, this hysteresis is shown as rate-dependent: its observed shape and width are influenced not only by the material intrinsic properties or the light intensity value but also by the temperature sweep rate. Therefore, one may measure an experimental light-induced thermal hysteresis even if the intermolecular interactions are so small that a thermal hysteresis is not visible—this hysteresis magnified by kinetic effects may be real or apparent.

In this paper, we investigate the light-induced thermal hysteresis of $\text{Fe}(\text{phen})_2(\text{NCS})_2$ (phen-1,10 phenanthroline) embedded in glycerol, a glassy matrix ($T_g = 194 \text{ K}$) [10], analyzing experimental data in the framework of an adapted mean-field model. It is already well-known for more than ten years that the thermal behavior considerably changes in nanoscale spin-crossover particles: smoother transition with narrower or even absent hysteresis, the shift of transition temperatures towards lower values, the existence of incomplete transitions [11–15]. Their incorporation in glassy matrices [16–19], which allows the stabilization of particles in a transparent medium and the tuning of optical characteristics, leads to even more spectacular features and sometimes to a larger hysteresis loop, of mechanical origin, due to the interactions between edge spin-crossover molecules and their environment.

In Figure 1 (left), one compares the major hysteresis thermal loop for $\text{Fe}(\text{phen})_2(\text{NCS})_2$ as polycrystalline powder (bare microparticles) and as dispersion of microcrystalline particles in glycerol, after a first cooling down followed by heating, up to 250 K. While in the case of the polycrystalline powder the thermal transition is accompanied by a 2 K hysteresis loop, microcrystals dispersed in glassy glycerol show a larger hysteresis loop of more than 50 K width, with a gradual HS–LS transition curve, shifted towards lower temperatures and an LS–HS transition curve quite similar to that observed for bare particles. However, no evidence for larger cooperativity was found, and the observations have been explained as a cutoff/switch-on mechanism of interactions between the spin-crossover microparticles and the surrounding matrix, determined by molecular volume change during the transition. We should emphasize that the cooperative hysteretic behavior observed in spin-crossover materials is a consequence of a high macroscopic energy barrier (formation of domains, first-order phase transition), raised by the elastic interactions in the hysteretic temperature range. In the microcrystals under investigation, the cooperativity is not high enough to promote such a regime, but the volume-dependent microcrystals–matrix interactions, which are specifically switched on and cutoff in the ascending and descending branch, respectively, impact the thermodynamical and kinetic characteristics of the spin-state switching. According to the size/volume ratio of particles, the microcrystals–matrix system becomes bistable with a new type of hysteretic behavior of mechanical origin.

Further experiments were focused on the study of photoexcitation and the relaxation of matrix embedded microcrystals. The conversion of $\text{Fe}(\text{phen})_2(\text{NCS})_2$ polycrystalline powder, detected as explained in the Materials and Methods section, is quite low (conversion around 20%) due to the bulk absorption of light. The dispersion of the powder of particles in glycerol, a fully transparent glassy matrix at low temperature, allows reaching a higher photoexcitation ratio (more than 50%) due to better transmission of the light. Typical relaxation curves for bare microparticles and microparticles embedded in glycerol presented in Figure 1 (right) show a self-accelerated process and a decrease of the apparent cooperativity resulting from embedding the particles in the surrounding environment,

which correspond to the smoother HS–LS transition in Figure 1 (left). This observation has been confirmed by a further classical mean-field treatment of experimental data, which presented a smaller cooperativity parameter, $\alpha = 1.55$ instead of the value of $\alpha = 2.5$ previously found for powder of microparticles [20]. At the same time, the activation energy stays constant at 800 K. This value is by far smaller than the threshold value of $\alpha = 4$ needed for the existence of a quasi-static hysteresis found in early papers discussing the LITH phenomenon [1,21].

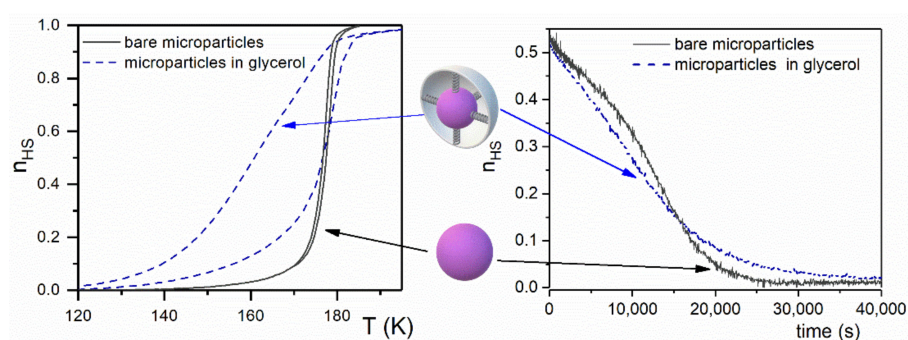


Figure 1. Thermal transition curves (left) and HS–LS relaxation curves measured in the dark at $T = 50$ K (right) for $\text{Fe}(\text{phen})_2(\text{NCS})_2$ as powder and as microparticles dispersed in glycerol.

The paper is organized as follows: first, we present experimental data showing the presence of a kinetic and quasi-static LITH, then we model the data in the framework of a mean-field model with negative variable pressure, and finally, we confirm the results using an Ising-like model for particles with Gaussian distributed sizes, embedded in frozen matrices.

2. Results

2.1. Light-Induced Thermal Hysteresis Experimental Results

In the main Figure 2, we present as black circles LITH data for $\text{Fe}(\text{phen})_2(\text{NCS})_2$ spin-crossover microparticles dispersed in glycerol (25 wt.%) corresponding to a temperature sweep rate of 0.3 K/min. As in the case of bulk compounds, the cooling branch is much more gradual than the warming branch due to the faster variation of relaxation rates at higher temperatures. The photoexcitation is uncompleted: based on previous photoexcitation results, we estimate that around half of the molecules are in the HS state at low temperatures. The small decrease of the χT at low temperature is due to the zero-field splitting in the HS quintet state. However, as we stated in the introduction, the simple observation of the kinetic “apparent” LITH does not imply that the “real” static hysteresis is also present. The real LITH would be obtained for an infinitely slow temperature sweep rate when the steady-state between photoexcitation and relaxation is achieved. To prove the existence of the real LITH loop, we have used here a method implemented previously by Létard et al. [22] and then verified for elastic model simulations [23]. This method is based on the measurement of relaxation curves under light starting from the two hysteretic branches. These relaxations under light are presented in the inset of Figure 2 at different temperatures: depending on the initial starting point, one or other steady states are obtained. As there is a gap between the curves obtained starting from HS and LS branches, we can conclude that a real quasi-static hysteresis exists, and its proposed profile is drawn in Figure 2 (main) with a dotted line. As expected, the real hysteresis is narrower than the apparent one (10 K width instead of 40 K width), keeping the asymmetry of a more gradual cooling branch.

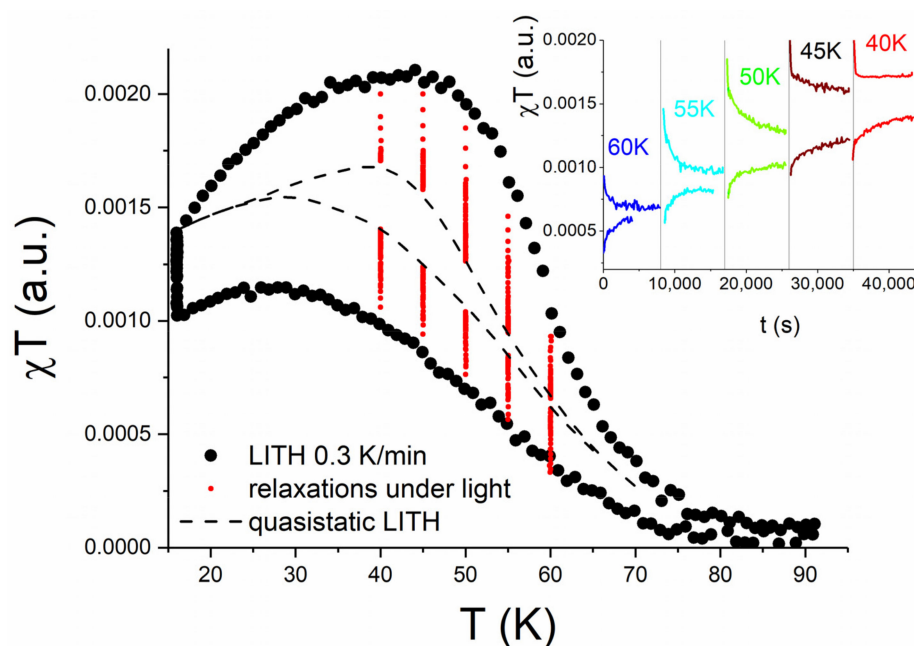


Figure 2. Light-induced thermal hysteresis for $\text{Fe}(\text{phen})_2(\text{NCS})_2$ microparticles embedded in glycerol (black circles experimental data measured at 0.3 K/min; red circles partial relaxation under light; dotted line: profile of the real LITH curve as a guide for the eye). (inset) Partial relaxation curves under light starting from the two hysteresis branches, showing the existence of a quasi-static real hysteresis.

2.2. Theory and Simulations

2.2.1. Mean-Field Model

The presence of a real LITH is unexpected as the value previously determined for the cooperativity coefficient α is too small to produce it. To understand this hardly predictable phenomenon, we propose here a model based on a mean-field classical master equation, including a photoexcitation and a relaxation term, and an additional term for pressure, which takes into account the influence of the frozen matrix on the spin-crossover microparticles. A similar equation was previously used to compute first-order reversal curves showing huge reversibility in the thermal hysteresis [17].

The master equation can be simply written as:

$$\frac{dn_{HS}}{dt} = I \cdot \sigma \cdot (1 - n_{HS}) - k_{HL}^{\infty} \cdot n_{HS} \cdot e^{-\frac{(E_A + \alpha \cdot T \cdot n_{HS} + p \Delta V_{HL})}{k_B T}} \quad (1)$$

where n_{HS} is the fraction of molecules in the HS state, $I \cdot \sigma$ is the product between the light intensity and the absorption cross-section, k_{HL}^{∞} is the HS–LS relaxation rate constant at $n_{HS} = 1$ and at very high temperature, E_A is the activation energy, p is the matrix-induced pressure, ΔV_{HL} the difference in unit cell volume per complex between the system in the two spin states, k_B the Boltzmann constant and T the temperature. In relation (1), $\alpha \cdot T$ is proportional to the interaction parameter in the statical description of thermal transition of spin-crossover compounds (usually denoted as Γ), as introduced by Spiering in his pioneering works. [24,25]

In the case of microparticles embedded in a matrix, the matrix-induced pressure is not constant but increases as the HS–LS transition proceeds. In a first approximation, we can consider a linear law:

$$p = p_0 + \beta(1 - n_{HS}) \text{ where } \beta > 0 \quad (2)$$

We should notice that β it acts in an opposite way compared to the cooperativity constant α , and its simple presence leads to a decrease of the cooperativity. The constant β depends on the particle size (as for larger microparticles, the negative pressure increases faster with diminishing n_{HS}), and therefore, according to experimental particle size distri-

bution, we can consider it as Gaussian with standard deviation σ_β and the average value $\bar{\beta}$. For the sake of simplicity, we allow the initial pressure applied by the matrix to the particle p_0 to be 0.

In Figure 3 (main), we present the major hysteresis loop under light (kinetic LITH), which fairly corresponds to experimental data. We have considered the parameters identified previously by analyzing relaxation curves $\alpha = 1.6$ and $E_A = 800$ K. The other parameters are $I\sigma = 0.0001 \text{ s}^{-1}$, $\bar{\beta} \cdot \Delta V_{HL} = 150$ K, $\sigma_\beta = 30$ K. However, as we explained before, the presence of a kinetic hysteresis does not imply that a real hysteresis exists. Therefore (as the presence of distributions β does not allow an exact computation of the quasi-static LITH), we reproduce, as in experiments, the partial relaxation curves under light starting from the two branches and observe that for every temperature, these curves join somewhere inside the hysteresis loops. This signifies that it is not possible to obtain real bistability under light if considering only a distribution of the variations of local pressures. Therefore, an additional hypothesis to understand the experimental bistability is needed.

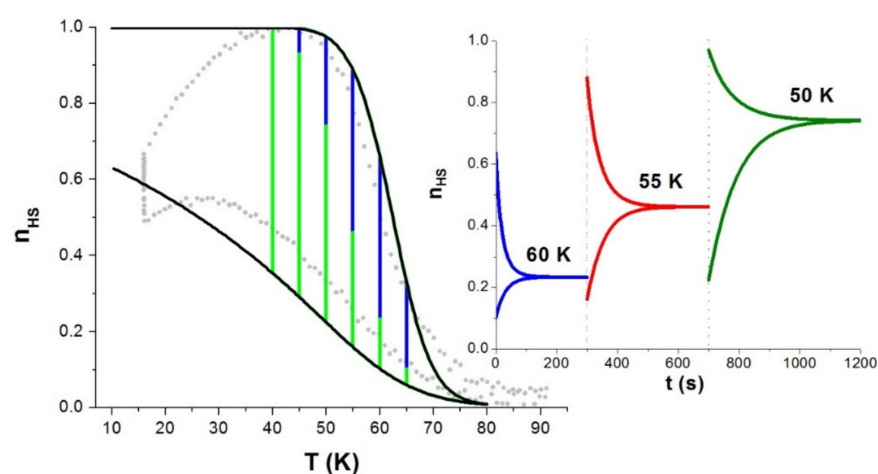


Figure 3. Light-induced thermal hysteresis simulated (black line) using Equation (1) with the variation of individual pressures on molecules described by Equation (2) considering a Gaussian distribution of pressure variation constant (black open circles; experimental data, blue and green lines: partial relaxation under light) and (inset) partial relaxation curves under light starting from the two hysteresis branches, showing the absence of a quasi-static real hysteresis.

Due to the change in volume of microparticles during the HS–LS transition, it is reasonable to suppose that at a certain moment, the distance between the matrix and the edges of the encapsulated spin-crossover microparticles becomes too large, and consequently, the negative pressure modulated by the environment does not follow the relation (2) anymore and goes slowly to zero; from this point on, the microparticles behave similarly to bare microparticles. They do the same when the LS–HS transition starts, but at a certain moment, when enough molecules have switched to the HS state, the volume of particles increase again, and the particles start to interact with the matrix (in the assumption of physisorption mediated by van der Waals forces). A similar “cutoff/switch-on” mechanism, illustrated in Figure 4, was used to explain the huge reversibility during the thermal transition of microparticles in glycerol [17].

Using these new assumptions, we have considered that if the pressure equalizes a threshold value ρ in the case of HS–LS transition, then the links with the environment vanish, and the pressure goes linearly to zero following the relation $p = \rho \cdot n_{HS} / n_{HS}^\rho$, with n_{HS}^ρ the HS fraction corresponding to the moment when the pressure becomes equal to ρ . Reversely, in the case of LS–HS transition, the pressure stays constant until n_{HS} equalizes n_{HS}^ρ then linearly increases, such as to recover its initial value for $n_{HS} = 1$. Consequently, these assumptions lead to different initial external conditions for HS–LS and LS–HS transitions. We should strengthen that n_{HS}^ρ value depends on β (smaller for

larger β values), and as β the coefficient is distributed, it is possible that in some cases, the threshold value is not be reached. In these situations, the pressure varies only according to relation (2). In Figure 5, we present the simulations obtained for $\rho\Delta V = 120K$ reproducing the LITH as in the experiment and the partial relaxation curves under the light. In this case, the relaxation curves are not joining in a large temperature range, so the non-cooperative mechanism induces real bistability in the system in the presence of a cutoff/switch-on mechanism.

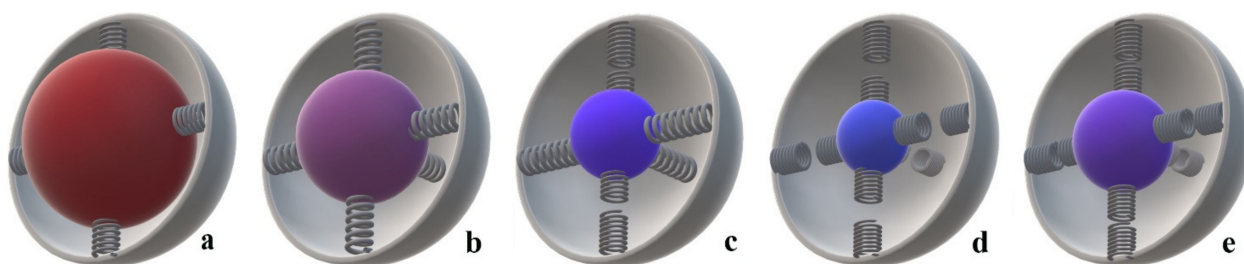


Figure 4. Schematic representation of the switch-on/cutoff mechanism. A spin-crossover particle in a matrix: the springs have their natural length—no initial pressure exerted on the central particle (a); upon the HS–LS transition, the particle size diminishes, the matrix-induced pressure progressively increases (b), and when the particle is too small its interaction with the matrix are progressively cut (c) and the pressure from the matrix goes to zero (cutoff; (d)); when the particle size increases again (LS–HS transition) the link between it and the matrix is rebuilt (switch-on; (e)).

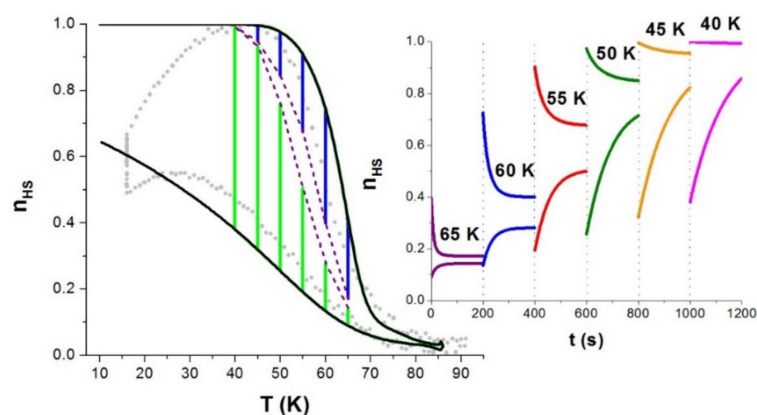


Figure 5. (left) Experimental data (circles) and simulations (black lines) in a framework of a mean-field approach with a switch-on/cutoff mechanism. Partial relaxation curves (blue and green lines) and the real LITH (dotted line—a guide for the eye). (right) Partial relaxation curves under light showing the existence of true bistability [18].

2.2.2. Ising-Like Model

To strengthen the results obtained using the mean-field approach, we have tested the same switch-on/cutoff hypothesis in the framework of an Ising-like model, which allows a more advanced analysis due to the explicit consideration of short-range interactions and, therefore, the study of either small-sized particles or of particles embedded in surfactant coating, for which molecules at the interface can play an important role during the transition.

The Ising model for spin-crossover complexes associates a fictitious spin ($\sigma_i = \pm 1$ i.e., HS $\rightarrow +1$ and LS $\rightarrow -1$ state) to each molecule situated in a rectangular configuration (see Figure 6) and introduces short- and long-range intermolecular interactions through the following Ising-like Hamiltonian:

$$H = \frac{1}{2} \sum_i (D - k_B T \ln g) \sigma_i - J \sum_{i,j} \sigma_i \sigma_j - G \sum_i \sigma_i \langle \sigma \rangle \quad (3)$$

with D and g as the energy difference and the degeneracy ratio between the two states, J is the short-range interaction and G the long-range interaction constants. The fraction n_{HS} is expressed as a function of the “fictitious magnetization” $n_{HS} = \frac{1+\langle\sigma\rangle}{2}$.

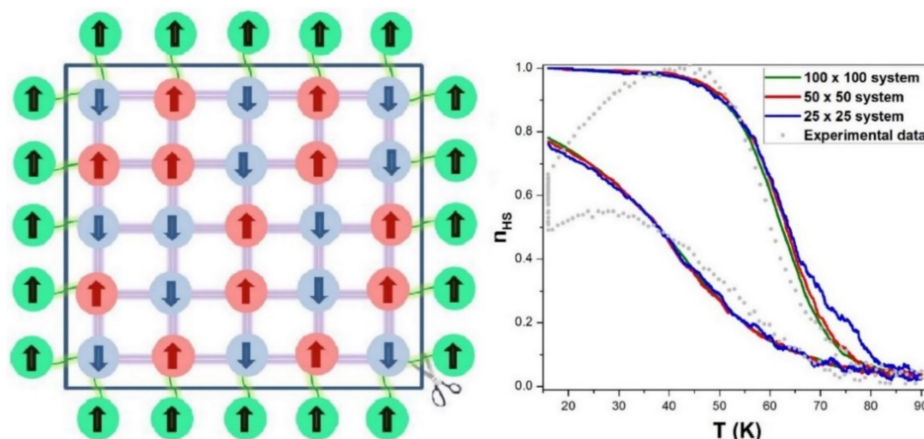


Figure 6. (left) Schematic representation of an Ising-like system containing HS (spin up—red molecules) and LS molecules (spin down—blue molecules) interacting with the HS environment, which can be cut, as explained in text; (right) LITH computed in the framework of an Ising-like model for different sizes considering a switch-on/cutoff mechanism.

In the Ising-like model, the intermolecular interactions play the role of internal pressure, which acts upon the molecular volume of the two species. To account for the interaction between spin-crossover particles and the environment, we have considered a surrounding layer of molecules in frozen HS states, interacting with edge spin-crossover molecules by a specific short-range interaction J' .

The evolution of the system follows Monte Carlo Arrhenius dynamics [26], in which the transition probabilities are modulated by the activation energy E_A .

$$\begin{aligned} P_{HS \rightarrow LS}^i &= \frac{1}{\tau} \exp\left(\frac{D - k_B T \ln g}{2k_B T}\right) \exp\left(-\frac{E_A + 2G\langle\sigma\rangle + 2J\sum\sigma_{neighbors}}{k_B T}\right) \\ P_{LS \rightarrow HS}^i &= I\sigma + \frac{1}{\tau} \exp\left(-\frac{D - k_B T \ln g}{2k_B T}\right) \exp\left(-\frac{E_A - 2G\langle\sigma\rangle - 2J\sum\sigma_{neighbors}}{k_B T}\right) \end{aligned} \quad (4)$$

where τ is a scaling constant. The term $\sum\sigma_{neighbors}$ is the sum of the fictitious spin values of the first-order neighbors of the molecules whose transition probability is calculated. When an edge molecule is under evaluation, short-range interaction J is replaced with the interaction constant J' to account for the interaction with the environment.

The Monte Carlo algorithm is the following: (1) We consider all the molecules in the HS (for heating LITH branch) or LS state (for cooling LITH branch); (2) For a randomly chosen molecule in the system, we calculate the transition probability; (3) If this probability is larger than a randomly generated number $r \in (0, 1)$, then the transition occurs and the particle switches to the new spin state; if it is smaller than r , the particle keeps its spin state; (4) We repeat the steps (2) and (3) for many molecules equal to all the particles in the system; this concludes a Monte Carlo Step (MCS). The number of MCSs achieved at each temperature controls the temperature sweep rate; more steps lead to a smaller hysteresis width, closer to the quasi-static one. Additionally, we should notice that even in the experiments, only around 50% of molecules were photoexcited due to the bulk absorption of light, and so the photoexcitation is nonhomogenous. In this case, it has been shown that the corresponding relaxation curves (and consequently LITH curves) are expected to be similar to the case of full photoexcitation [23]. Therefore, in the present model, we may assume that all the molecules are in the HS state at the beginning of the heating LITH branch without influencing the interpretation of results.

In Figure 7 we have represented relaxation curves under light for two different size systems (50×50 and 100×100) using the following parameters $E_A = 800$ K, $\Delta = 1000$ K,

$\Delta S = 5$ K, $J = 1.5$ K, $G = 10$ K, $\tau = 0.07$, $I\omega = 0.001$. For a constant value of $J' = 10$ K, no quasi-static hysteresis is observed (Figure 7 (left)); the same is the case for all tested values of J' . Next, a switch-on/cutoff mechanism was added to the model using the following approach: during the HS–LS transition, as long as more than γ % of the molecules are in the HS state, J' stays constant. Subsequently, the value of J' decreases linearly to zero with the value of n_{HS} , which is similar to the mean-field approach. During the LS–HS transition, in the beginning, there are no interactions between environment molecules and spin-crossover edge molecules, but they start to buildup progressively as the transition proceeds and n_{HS} surpasses a threshold. The results in Figure 7 show that a quasi-static hysteresis can be obtained only in the framework of a cutoff/switch-on mechanism (we have considered here $\gamma = 50\%$, but similar results can be obtained for other values γ). However, once the system size increases (for example, 100×100 molecules), the width of the LITH diminish since the ratio edge molecules/total number of molecules decreases. Nevertheless, this feature can be attenuated if considering second or higher-order neighbors.

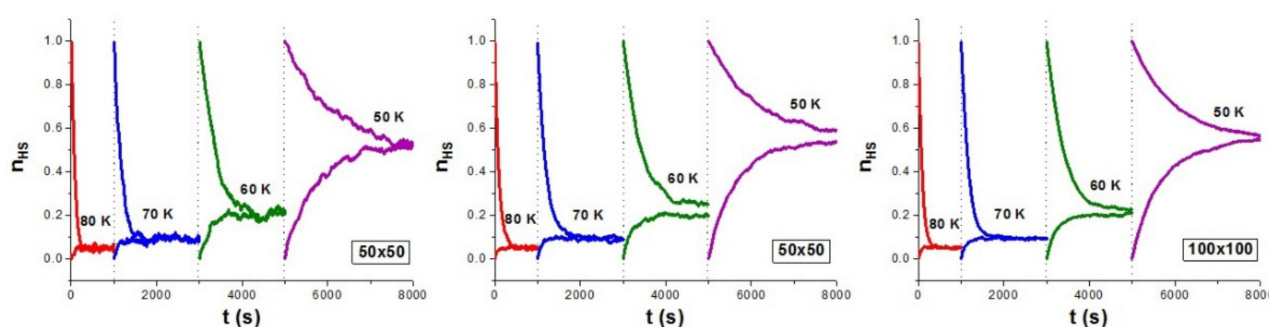


Figure 7. Relaxation curves under light for systems composed of 2500 molecules (50×50) with a constant interaction coefficient with the environment (no quasi-static hysteresis loop) (left) and considering a cutoff/switch-on mechanism (middle). In the case of a larger system of 10,000 molecules (right), there is no real hysteresis even if the cutoff/switch-on mechanism is considered, as the ratio edge molecules/total number of molecules is too low.

In a further development of the model, for a closer link to physical spin-crossover material, we have considered the Gaussian distribution of particle sizes. It is centered on particles with 30 molecules on every side and a standard deviation of 7 molecules. In Figure 8, we present these results as averaged LITH, including the quasi-static loop resulting from partial relaxations under the light.

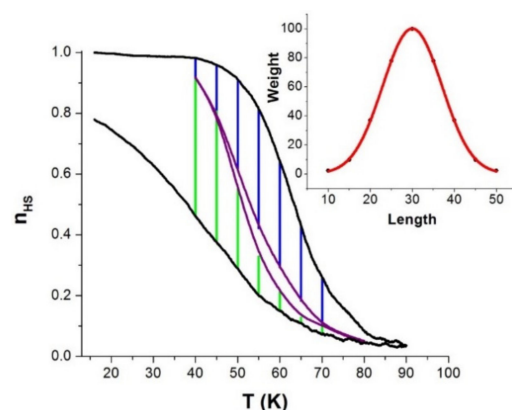


Figure 8. Kinetic LITH and real LITH computed using relaxation curves under light for a Gaussian distribution of particles (in the inset) considering a switch-on/cutoff mechanism.

2.3. First-Order Reversal Curves and Their Interpretation

The in-depth analysis of the distributions involved in the appearance of a real or kinetic hysteresis can be realized by measuring the so-called first-order reversal curves

(FORC) [10,27,28]. These are a specific class of minor hysteresis loops, for which the sweep of the input parameter, the temperature here, is reversed once starting from specific points on the major hysteresis loop.

A cooling LITH FORC measurement starts at a sufficiently high temperature, where all molecules are in their stable LS states. Then the temperature is decreased to a reversal temperature T_R . Subsequently, the temperature is raised, and the parameter of interest, n_{HS} in our case, is measured at an actual temperature T . A similar procedure is considered for the heating mode.

To obtain the FORC distribution and its corresponding diagram, several FORCs are measured for different reversal temperatures T_R . A FORC distribution is simply defined as the second-order mixed derivative of the n_{HS} parameter:

$$\rho(T, T_R) = \pm \frac{\partial^2 n_{HS}}{\partial T \partial T_R} \quad (5)$$

where the negative sign is for the cooling mode and the positive sign is for the heating mode.

The FORCs for the cooling and heating modes are presented in Figure 9. A quick inspection of the FORCs shows the kinetic behavior of the system. The n_{HS} fraction on a cooling FORC first increases as the system aims towards the stationary state under the light. This occurs at a higher n_{HS} than the measured one because of the finite experimental time, which is smaller than the relaxation time. Then, after reaching the plateau, the n_{HS} decreases towards the LITH hysteresis branch. This is a generic feature of FORC experiments for which the evolution rate of the system is dependent on the temperature scan rate.

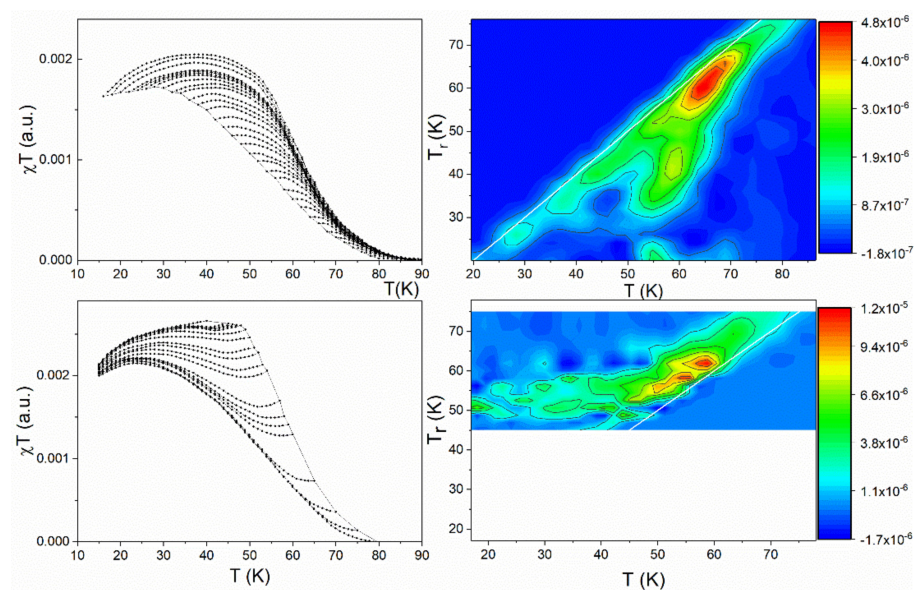


Figure 9. FORCs and FORC distributions for $\text{Fe}(\text{phen})_2(\text{NCS})_2$ microparticles embedded in glycerol for heating (lower side) and cooling modes (upper side).

The kinetic effects are visible on the two FORC diagrams. We notice the existence of two distributions: a negative one situated along the reversal temperature line, i.e., the first bisector, which is fully kinetic and a positive one in the central part of the two diagrams. This central distribution should correspond to the temperature distribution (determined by size or interaction distributions determined by the cutoff/switch-on mechanisms as explained in previous paragraphs).

3. Discussion

The dispersion of $\text{Fe}(\text{phen})_2(\text{NCS})_2$ in a glassy glycerol matrix allows the observation not only of larger thermal hysteresis compared to the neat compound but also of unexpected real light-induced thermal hysteresis. This hysteresis is not due to intrinsic cooperative

effects, which are lower than the threshold needed for obtaining a static LITH, but merely originate in the variable mechanical stress between spin-crossover microparticles and glycerol environment. The two models presented in this paper show the necessity of considering a variable pressure and a switch-on/cutoff mechanism for reproducing the quasi-static real hysteresis with experimental parameters. In future works, the Ising-like model can be extended through an elastic approach, which should allow a finer study of the dependence of external pressure on the size of the spin-crossover particle.

4. Materials and Methods

MP glycerol $((1600 \pm 600) \times (1600 \pm 600) \times (300 \pm 200) \text{ nm}^3)$ of $\text{Fe}(\text{phen})_2(\text{NCS})_2$ was synthesized according to a procedure described in [29] and then dispersed [19] in glycerol (glass transition temperature $T_g \approx 185\text{--}192 \text{ K}$) [30] with a percentage of 25% spin active compound concerning the dispersant. Around 2 mg of this mixture were set in a small sample holder at the end output of the optical fiber.

Experimental LITH for $\text{Fe}(\text{phen})_2(\text{NCS})_2$ spin-crossover microparticles dispersed in glycerol (25 wt %) was recorded using the “sweep” function of the SQUID magnetometer equipped with an optical fiber to ensure a constant temperature sweeping rate. The magnetic moment was measured at a constant magnetic field (5000 Oe) and provided a signal proportional to the HS population. The irradiation was performed using a continuous green laser (532 nm) with a power density of $2 \text{ mW}/\text{mm}^2$. The FORCs were recorded in the same experimental conditions as LITH, considering a temperature difference of 1 K between two consecutive reversal curves.

Author Contributions: Conceptualization, M.-L.B. and C.E.; methodology, R.T., M.-L.B. and C.E.; sample preparation, J.L. and M.-L.B.; software, D.P., A.R. and C.E.; Experiments, R.T. and C.E.; FORC data treatment, R.T. and A.S.; writing—original draft preparation, C.E., writing—review and editing, R.T., M.-L.B. and C.E. All authors have read and agreed to the published version of the manuscript.

Funding: This work was supported by a grant from the Romanian Ministry of Education and Research, CNCS—UEFISCDI, project number PN-III-P4-ID-PCE-2020-1946, within PNCDI III. The collaboration between Romanian and French teams was supported by the PHC Brancusi program.

Conflicts of Interest: The authors declare no conflict of interest.

References

1. Desaix, A.; Roubeau, O.; Jeffic, J.; Haasnoot, J.G.; Boukheddaden, K.; Codjovi, E.; Linares, J.; Nogues, M.; Varret, F. Light-induced bistability in spin transition solids leading to thermal and optical hysteresis. *Eur. Phys. J. B* **1998**, *6*, 183–193. [[CrossRef](#)]
2. Létard, J.F.; Guionneau, P.; Rabardel, L.; Howard, J.A.K.; Goeta, A.E.; Chasseau, D.; Kahn, O. Structural, magnetic, and photo-magnetic studies of a mononuclear iron(II) derivative exhibiting an exceptionally abrupt spin transition. Light-induced thermal hysteresis phenomenon. *Inorg. Chem.* **1998**, *37*, 4432–4441. [[CrossRef](#)] [[PubMed](#)]
3. Hinek, R.; Spiering, H.; Gülich, P.; Hauser, A. The $[\text{Fe}(\text{etz})_6](\text{BF}_4)_2$ spin-crossover system—Part two: Hysteresis in the LIESST regime. *Chem. Eur. J.* **1996**, *2*, 1435–1439. [[CrossRef](#)]
4. Linares, J.; Codjovi, E.; Garcia, Y. Pressure and Temperature Spin Crossover Sensors with Optical Detection. *Sensors* **2012**, *12*, 4479–4492. [[CrossRef](#)] [[PubMed](#)]
5. Decurtins, S.; Gülich, P.; Kohler, C.P.; Spiering, H.; Hauser, A. Light-induced excited spin state trapping in a transition-metal complex: The hexa-1-propyltetrazole-iron (II) tetrafluoroborate spin-crossover system. *Chem. Phys. Lett.* **1984**, *10*, 1–4. [[CrossRef](#)]
6. Hauser, A. Light-induced spin crossover and the high-spin \rightarrow low-spin relaxation, in: Spin crossover in transition metal compounds II. *Top. Curr. Chem.* **2004**, *234*, 155–198. [[CrossRef](#)]
7. Hauser, A. High-Spin—Low-Spin Relaxation Kinetics and Cooperative Effects in the $[\text{Fe}(\text{ptz})_6](\text{BF}_4)$ and $[\text{Zn}_{1-x}\text{Fe}_x(\text{ptz})_6](\text{BF}_4)_2$ (ptz = 1-Propyltetrazole) Spin-Crossover Systems. *Inorg. Chem.* **1986**, *25*, 4245–4248. [[CrossRef](#)]
8. Varret, F.; Boukheddaden, K.; Codjovi, E.; Enachescu, C.; Linares, J. On the competition between relaxation and photoexcitations in spin crossover solids under continuous irradiation, in: Spin crossover in transition metal compounds II. *Top. Curr. Chem.* **2004**, *234*, 199–229. [[CrossRef](#)]
9. Chakraborty, P.; Enachescu, C.; Walder, C.; Bronisz, R.; Hauser, A. Thermal and Light-Induced Spin Switching Dynamics in the 2D Coordination Network of $\{\text{Zn}_{1-x}\text{Fe}_x(\text{bbtr})_3(\text{ClO}_4)_2\}_\infty$: The Role of Cooperative Effects. *Inorg. Chem.* **2012**, *51*, 9714–9722. [[CrossRef](#)]

10. Tanasa, R.; Enachescu, C.; Laisney, J.; Morineau, D.; Stancu, A.; Boillot, M.L. Unraveling the Environment Influence in Bistable Spin-Crossover Particles Using Magnetometric and Calorimetric First-Order Reverse Curves. *J. Phys. Chem. C* **2019**, *123*, 10120–10129. [[CrossRef](#)]
11. Volatron, F.; Catala, L.; Rivière, E.; Gloter, A.; Stephan, O.; Mallah, T. Spin-Crossover Coordination Nanoparticles. *Inorg. Chem.* **2008**, *47*, 6584. [[CrossRef](#)] [[PubMed](#)]
12. Gruber, M.; Berndt, R. Spin-Crossover Complexes in Direct Contact with Surfaces. *Magnechemistry* **2020**, *6*, 35. [[CrossRef](#)]
13. Laisney, J.; Morineau, D.; Enachescu, C.; Tanasa, R.; Rivière, E.; Guillot, R.; Boillot, M.L. Mechanical-tuning of the cooperativity of SC particles via the matrix crystallization and related size effects. *J. Mater. Chem. C* **2020**, *8*, 7067–7078. [[CrossRef](#)]
14. Boldog, I.; Gaspar, A.B.; Martinez, V.; Pardo-Ibanez, P.; Ksenofontov, V.; Bhattacharjee, A.; Gütlich, P.; Real, J.A. Spin-crossover nanocrystals with magnetic, optical, and structural bistability near room temperature. *Angew. Chem. Int. Ed.* **2008**, *47*, 6433. [[CrossRef](#)]
15. Félix, G.; Mikolasek, M.; Molnar, G.; Nicolazzi, W.; Bousseksou, A. Tuning the spin crossover in nano-objects: From hollow to core-shell particles. *Chem. Phys. Lett.* **2014**, *607*, 10–14. [[CrossRef](#)]
16. Raza, Y.; Volatron, F.; Moldovan, S.; Ersen, O.; Huc, V.; Martini, C.; Brisset, F.; Gloter, A.; Stephan, O.; Bousseksou, A.; et al. Matrix-dependent cooperativity in spin crossover Fe(pyrazine)Pt(CN)₄ nanoparticles. *Chem. Commun.* **2011**, *47*, 11501–11503. [[CrossRef](#)]
17. Tanasa, R.; Laisney, J.; Stancu, A.; Boillot, M.L.; Enachescu, C. Hysteretic behavior of Fe(phen)₂(NCS)₂ spin-transition microparticles vs. the environment: A huge reversible component resolved by first order reversal curves. *Appl. Phys. Lett.* **2014**, *104*, 031909. [[CrossRef](#)]
18. Enachescu, C.; Tanasa, R.; Stancu, A.; Tissot, A.; Laisney, J.; Boillot, M.L. Matrix-assisted relaxation in Fe(phen)₂(NCS)₂ spin-crossover microparticles, experimental and theoretical investigations. *Appl. Phys. Lett.* **2016**, *109*, 031908. [[CrossRef](#)]
19. Tissot, A.; Enachescu, C.; Boillot, M.L. Control of the thermal hysteresis of the prototypal spin-transition Fe_{II}(phen)₂(NCS)₂ compound via the microcrystallites environment: Experiments and mechanoelastic model. *J. Mater. Chem.* **2012**, *22*, 20451–20457. [[CrossRef](#)]
20. Balde, C.; Desplanches, C.; Nguyen, O.; Létard, J.F. Complete temperature study of the relaxation from HS to LS state in the mixed [Fe_xZn_{1-x}(phen)₂(NCS)₂] systems (with x = 1, 0.73, 0.5, 0.32, 0.19 and 0.04). *J. Phys. Conf. Ser.* **2009**, *148*. [[CrossRef](#)]
21. Roubeau, O.; Haasnoot, J.G.; Linares, J.; Varret, F. Inhomogeneous effects in the light-induced bistability and non-linear relaxation of cooperative spin-crossover solids. *Mol. Cryst. Liq. Cryst. Sci. Technol. Sect. A-Mol. Cryst. Liq. Cryst.* **1999**, *335*, 541–550. [[CrossRef](#)]
22. Letard, J.F.; Chastanet, G.; Nguyen, O.; Marcen, S.; Marchivie, M.; Guionneau, P.; Chasseau, D.; Gütlich, P. Spin crossover properties of the Fe(PM-BiA)₂(NCS)₂ complex—Phases I and II. *Mon. Chem.* **2003**, *134*, 165–182. [[CrossRef](#)]
23. Enachescu, C.; Stoleriu, L.; Stancu, A.; Hauser, A. Competition between photoexcitation and relaxation in spin-crossover complexes in the frame of a mechanoelastic model. *Phys. Rev. B* **2010**, *82*, 104114. [[CrossRef](#)]
24. Spiering, H.; Willenbacher, N. Elastic interaction of high-spin and low-spin complex molecules in spin-crossover compounds. II. *J. Phys. Condens. Matter* **1989**, *1*, 10089–10105. [[CrossRef](#)]
25. Gütlich, P.; Hauser, A.; Spiering, H. Thermal and optical switching of iron(II) complexes. *Angew. Chem. Int. Ed.* **1994**, *33*, 2024–2054. [[CrossRef](#)]
26. Krivokapic, I.; Enachescu, C.; Bronisz, R.; Hauser, A. Spin transition and relaxation dynamics coupled to a crystallographic phase transition in a polymeric iron(II) spin-crossover system. *Chem. Phys. Lett.* **2008**, *455*, 192. [[CrossRef](#)]
27. Enachescu, C.; Tanasa, R.; Stancu, A.; Codjovi, E.; Linares, J.; Varret, F. FORC method applied to the thermal hysteresis of spin transition solids: First approach of static and kinetic properties. *Physica B* **2004**, *343*, 15–19. [[CrossRef](#)]
28. Enachescu, C.; Tanasa, R.; Stancu, A.; Varret, F.; Linares, J.; Codjovi, E. First-order reversal curves analysis of rate-dependent hysteresis: The example of light-induced thermal hysteresis in a spin-crossover solid. *Phys. Rev. B* **2005**, *72*, 054413. [[CrossRef](#)]
29. Laisney, J.; Tissot, A.; Molnar, G.; Rechinat, L.; Rivière, E.; Brisset, F.; Bousseksou, A.; Boillot, M.L. Nanocrystals of Fe(phen)₂(NCS)₂ and the size-dependent spin-crossover characteristics. *Dalton Trans.* **2015**, *44*, 17302–17311. [[CrossRef](#)]
30. Chelli, R.; Procacci, P.; Cardini, G.; Della Valle, R.G.; Califano, S. Glycerol condensed phases Part I. A molecular dynamics study. *Phys. Chem. Chem. Phys.* **1999**, *1*, 871. [[CrossRef](#)]